

HASSAN, A., KHAN, M.A., YOUNAS, M., JAFFERY, S.H.I., KHAN, M., AHMED, N. and AWANG, M. 2024. Impact of dry and cryogenic cutting medium on shear angle and chip morphology in high-speed machining of titanium alloy (Ti-6Al-4V). *International journal of automotive and mechanical engineering* [online], 21(2), pages 11316-11331. Available from: <https://doi.org/10.15282/ijame.21.2.2024.11.0874>

# Impact of dry and cryogenic cutting medium on shear angle and chip morphology in high-speed machining of titanium alloy (Ti-6Al-4V).

HASSAN, A., KHAN, M.A., YOUNAS, M., JAFFERY, S.H.I., KHAN, M., AHMED, N. and AWANG, M.

2024

© 2024 The Author(s). Published by Universiti Malaysia Pahang Al-Sultan Abdullah Publishing. This is an open access article under the CC BY-NC 4.0 International license.

## RESEARCH ARTICLE

# Impact of Dry and Cryogenic Cutting Medium on Shear Angle and Chip Morphology in High-speed Machining of Titanium Alloy (Ti-6Al-4V)

Adeel Hassan<sup>1,2\*</sup>, Muhammad Ali Khan<sup>2,3</sup>, Muhammad Younas<sup>4</sup>, Syed Huasin Imran Jaffery<sup>2</sup>, Mushtaq Khan<sup>5</sup>, Naveed Ahmed<sup>6</sup>, Mokhtar Awang<sup>1</sup>

<sup>1</sup>Department of Mechanical Engineering, Universiti Teknologi PETRONAS, Seri Iskandar 32610, Perak Darul Ridzuan, Malaysia

<sup>2</sup>Department of Design and Manufacturing Engineering, School of Mechanical and Manufacturing Engineering, National University of Sciences and Technology, Sector H-12, Islamabad 44000, Pakistan

<sup>3</sup>Department of Mechanical Engineering, College of Electrical and Mechanical Engineering, National University of Sciences and Technology, Sector H-12, Islamabad 44000, Pakistan

<sup>4</sup>School of Engineering, Robert Gordon University, Aberdeen, United Kingdom

<sup>5</sup>Mechanical Engineering Department, Prince Mohammad Bin Fahd University, AL-Khobar 31952, Saudi Arabia

<sup>6</sup>Department of Industrial Engineering, College of Engineering and Architecture, Al-Yamamah University, Riyadh 11512, Saudi Arabia

**ABSTRACT** - Ti-6Al-4V, a titanium alloy, is widely employed in various engineering sectors due to its attractive combination of strong corrosion resistance and specific strength. However, titanium alloys frequently result in serrated chips, which present considerable machinability issues compared to other materials. The cutting medium plays a vital role in the chip formation mechanism, further affecting the machined part integrity and thermo-mechanical properties. Chip morphological parameters such as shear angle, compression ratio, and segmentation degree are essential aspects of estimating machined part surface roughness, tool wear, cutting forces, and energy consumption. Therefore, it is important to understand the entire mechanism of chip formation in terms of chip morphology in high-speed cutting. This fundamental research aims to analyze and compare the shear angle model and chip formation of titanium alloy Ti-6Al-4V for cutting speeds ranging from 50 m/min to 150 m/min and feed rates ranging from 0.12 mm/rev to 0.24 mm/rev under dry and cryogenic cutting environments. Single-point turning experiments were conducted on Ti-6Al-4V workpieces with uncoated tungsten carbide inserts (without chip breakers), which are advantageous for heat transfer. After the chip analysis, it was observed that the shear angle obtained practically with model-4 is the most appropriate model for shear angle calculation, and the cryogenic cutting medium is suitable for Ti-6Al-4V machining. At the feed rate of 0.12-0.24 mm/rev and cutting speed of 50-150 m/min, the shear angle in dry-medium machining ranges from 32° to 42°, while in cryogenic medium machining, it ranges from 34.6° to 44.6°. Overall, a larger shear angle has been observed in cryogenic turning compared to dry turning, which is advantageous for reduced cutting forces owing to a lesser shear plane. The tool-chip contact length, which is the intimate contact between the tool face and chip surface, significantly decreases under cryogenic media. A smaller tool-chip contact length results in an elevated shear angle, which improves process sustainability and economy during cryogenic turning, as described.

## ARTICLE HISTORY

Received : 24<sup>th</sup> Oct. 2023

Revised : 03<sup>rd</sup> Apr. 2024

Accepted : 27<sup>th</sup> May 2024

Published : 20<sup>th</sup> June 2024

## KEYWORDS

*Titanium alloy*

*Ti-6Al-4V*

*Shear angle*

*Chip morphology*

*Dry and cryogenic machining*

## 1.0 INTRODUCTION

Economics, environment and social sustainability are the three main stones of the sustainability foundation, which can be achieved by minimizing the machine tool's energy utilization and improving the cutting tool's life [1], [2]. In manufacturing industries, the electrical energy consumed in the machining process contributes significantly to the overall energy used [3]. In the industry, the machining operation is mainly utilized to get the desired part, having a designed geometric configuration and surface finish after removing the unwanted material with the help of a cutting tool from the initial raw material. The undesirable material is removed in the form of chips. The energy spent on the tool-chip interface while removing a specific volume of a material is commonly called Specific Cutting Energy (SCE) and is based on machining conditions and the type of chips produced [4], [5]. There are three basic types of chips (shown in Figure 1): continuous without build-up-edge (BUE), continuous with BUE, and serrated or segmented chips. The continuous chips are produced during the turning of ductile material under proper conditions, while the build-up-edge (BUE) is produced during the turning of difficult-to-cut material to break the chips. However, the particles of the cutting tool's BUE may deposit on the freshly machined surface. Segmented chips are produced in the machining of titanium alloys and lead to a reduction in tool life and poor surface finish, which ties up to an increase in the energy needed and less mechanical efficiency of the machined parts [6].

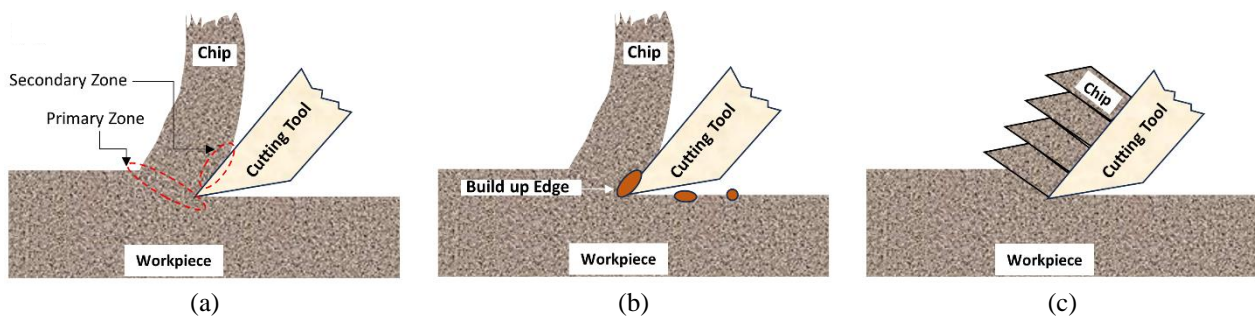


Figure 1. Types of chips: (a) continuous chip without BUE; (b) continuous chip with BUE; (c) segmented chips

Titanium alloys are classified as  $\alpha$  alloys, near  $\alpha$ ,  $\alpha$ - $\beta$  alloys, and  $\beta$  alloys, and Ti-6Al-4V is an  $\alpha$ - $\beta$  alloy (Grade 5) that has high-ranking properties at elevated temperatures, such as high fatigue, corrosion and strength resistance among these alloys. This alloy is a highly versatile titanium alloy and is utilized across multiple industries: aerospace, for airframes, landing gear, and engine components, including turbine blades and compressor parts; marine applications, such as propeller shafts, hulls, and underwater structures; and biomedical fields, for knee joints, bone plates, and spinal fusion cages [7], [8]. Ti-6Al-4V is lighter in weight as compared to steel and offers the benefits of lower fuel consumption and efficient working at high temperatures in jet engines. Due to this, 40% of this alloy is consuming the aeronautical industry to fabricate engine structures or parts either alone or in fiber metal laminate structure [9],[10]. Apart from its good mechanical properties, this alloy is considered difficult to cut alloy on account of its high chemical reactivity, low elastic resistance, and low thermal conductivity [11]. Tool and work-piece interaction during machining is more chemical in nature, which makes Ti-6Al-4V alloy hard to cut. The critical challenges of machining this alloy are tool life, energy consumption, and surface quality, which still need to be overcome [12],[13],[14]. High-speed machining (HSM) is basically the cutting speed above which complete shear localization is established in the primary shear zone that has developed immense interest among the research community to increase the machining efficiency of Ti-6Al-4V alloy [15], [16]. In the machining of titanium alloy, the primary shear zone is where the primary deformation of the workpiece begins, experiencing significant deformation. Conversely, the secondary zone is where the chip undergoes further deformation and segmentation, as illustrated in Figure 1 and Figure 2. The secondary zone plays a crucial role in determining the final chip morphology. The high-speed machining range for titanium alloys begins from 100 m/min, which is a relatively low speed [17].

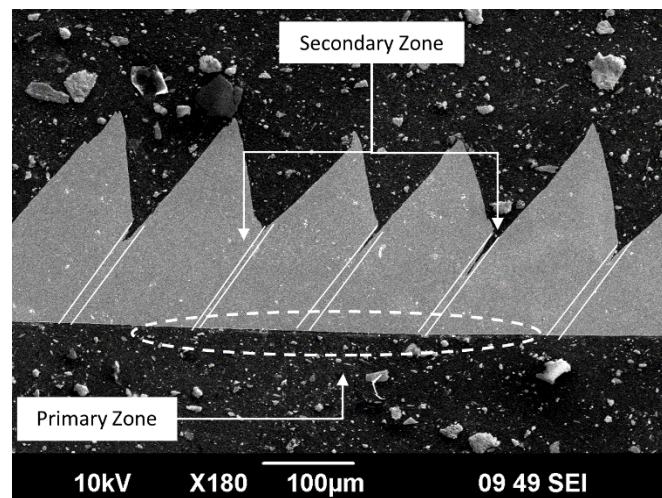


Figure 2. SEM image of segmented chips achieved in the present study indicates primary and secondary zones

Finally, serrated chips, also known as saw teeth, produced during the machining of titanium alloy at relatively low cutting speeds, lead to variation in the cutting forces and tool vibration, resulting in tool failure and more energy consumption. There are two main well-known theories that explain segmented chip formation: adiabatic shear theory and periodic crack theory [18]. According to the adiabatic theory, the thermoplastic shear instability happens in the primary shear zone, which is the root cause of serrated chip formation. It is believed that thermoplastic instability starts when the thermal softening rate exceeds the strain and strain hardening. This theory is supported by Semiatin [19], Molinari et al. [20], Sutter [21], Joshi et al. [22] and Komanduri et al. [23]. On the other hand, the periodic crack theory proposes that segments are formed due to the initiation of cracks periodically from the chip's free surface, which further propagates to the tool tip that weakens the adiabatic shear. This theory was campaigned by Nakayama et al. Vyas, Elbestawi et al. [24]–[26]. Overall, the discrepancy between these two theories is whether the slide surface of the segment is due to the adiabatic shear or not. Nevertheless, this mechanism is not fully comprehended [27].

In orthogonal cutting, chip morphological parameters comprise shear angle, chip peak and valley height, crack pitch, tooth pitch, equivalent deform thickness or segment length, shrinkage factor, and segmentation degree, etc., are essential features to estimate process stability in terms of the machined part integrity, cutting forces, tool wear and energy consumed [28]. The shear angle ( $\phi$ ) is the angle between the shear plane and the surface of the workpiece or cutting velocity, which is helpful in understanding the mechanism of chip formation. It is the evidence of the facility with which the material is cut as lower cutting temperature, lower power requirement, and lower specific shearing energy are the benefits of a higher shear angle [29]. A high shear angle yields low cutting temperature and, consequently, less tool wear, which reduces the chances of residual stresses and results in improved fatigue life, dimensional stability, and overall mechanical performance of the parts. This important morphological parameter is generally calculated theoretically using a function of chip thickness ratio (ratio of undeformed chip thickness to deformed or actual chip thickness) and practically using chip complementary angle. For theoretical calculations, a single-point turning operation assumes that the undeformed thickness is equal to the tool feed rate. However, the challenge lies in accurately calculating the actual chip thickness. Using a micrometer may not be the best approach to tackle this issue due to the rough back of the machined chip, which can yield inaccurate results [30]. The average chip thickness that is commonly measured with a micrometer shows a variation of 10 % to 25 % from their mean values [31]. So, appropriately mounted and ground samples of chips can be analyzed under a metallographic microscope to measure chip thickness accurately. However, the problem remains unsolved, as there are some controversial views that exist in which geometric parameters are considered for segmented chips, either by means of peak and valley height or segment length, which is used as deformed thickness.

Numerous studies have been published that analytically examined the Ti-6Al-4V alloy chip shape and production mechanism and created theoretical models [32], [33]. Regardless, numerous interacting variables in the chip development process make the analytical studies more complex for application. There is a need for the application of simplifications that frequently result in inaccurate estimates of various chip-geometric parameters [34]–[36]. Other studies numerically investigate the serrated chips mechanism using finite element (FE) methods [36]–[42]. The usefulness of these models is limited when the governing laws of the materials being used (tools and workpieces) are not well established. This often results in inaccurate estimation of certain chip geometric parameters [34],[43]. Experimental studies to calculate chip morphological parameters were also carried out by real-time image/video capturing and using metallographic procedures (hot mounting, grinding/polishing and chemical etching) along with optical microscopy or scanning electron microscopy (SEM). After that, digitally captured images are imported into the image processing software to calculate the chip's geometric parameters. Many studies have been done to investigate the effect of the most common machining parameters, such as cutting speed and tool feed rate, on the morphology of the segmented chip. The main issue is with the estimating of a critical geometric parameter, which is the shear angle. As already discussed, it is the relation between deformed (actual thickness) and un-deformed chip (feed rate) thickness and the issue is regarding the consideration of the actual chip thickness after the cut. Either it will be a segment length or mean of peak and valley height. So, in this regard, there are four main shear angle calculation methods/models that are being used by most of the researchers for estimation, which are contrasted below in Table 1, along with cutting material and environment.

Table 1. Summary of shear models

	Shear Angle Model	Type of Process and Work Piece Material	Ref.
Model-1	Chip Thickness Ratio: $r = \frac{Pc}{P}$ Shear Angle: $\phi = \tan^{-1}(r)$ Where, $P_c$ is tooth's pitch and $P$ is crack pitch	Dry-Turning Carburized steel, Ti-6Al-4V	[44] , [45]
Model-2	Chip Thickness Ratio: $r = \frac{h_1}{h_2}$ Shear Angle: $\phi = \tan^{-1}(r)$ where $h_1$ is undeformed thickness, which is equal to feed rate in single point turning, and $h_2$ is after cut thickness, which is chip segment length	Dry-Turning Ti-6Al-4V, AISI 1045 steel	[46], [47]
Model-3	Chip Thickness Ratio: $r = \frac{t_0}{t_c}$ $t_c = \frac{h_p+h_v}{2}$ Shear Angle: $\phi = \tan^{-1}(r)$ $t_0$ is feed rate and $t_c$ is the actual chip thickness (mean value of chip tooth's peak and valley)	Dry-Turning Ti-6Al-4V	[34], [48]–[51]
Model-4	Shear Angle: $\phi = \frac{\pi}{2} - \theta'$ where, $\theta'$ is segment angle	Dry-Turning Ti-6Al-4V	[52]–[56]

Thus, from the literature study, it is clear that four methods or models are being used to estimate the shear plane angle for serrated chips (shown in Table 1). The first three models are developed based on chip thickness ratio in terms of pitch ratio or tooth mean height, and it is supposed that a continuous chip is produced when calculating the chip thickness ratio. These models are theoretical models. Model 4 is a practical model based on the experimentally measured angle by

subtracting the segment complementary angle from  $90^\circ$ . On the other hand, segmented chips produced under a cryogenic cutting environment were not morphologically assessed in a cryogenic environment. Thus, there is a need to research which model and cutting medium is the most suitable for shear plane angle and compression ratio. This can contribute to the development of an SCE map and wear map (interlinked with temperature and residual stresses distribution), which may further help the shop floor to achieve dimensionally precise and mechanically efficient parts.

## 2.0 METHOD AND MATERIALS

A solid bar of aerospace titanium alloy Ti-6Al-4V (Grade 5) was selected as a workpiece material. The chemical composition (% weight) of the selected alloy is shown in Table 2. The turning experiments were carried out using a computer numerically controlled (CNC) turning machine with the characteristics indicated in Table 3, both in dry and cryogenic environments. Conventional coolant systems and MQL present several challenges, including increased cutting forces resulting in reduced sustainability and high disposal costs. Similarly, chilled air throw can result in uneven cooling across the workpiece and cutting tool, adversely affecting surface finish and tool life. As a result, these conditions were not included in the present study [57]. Thus, in this study, liquid nitrogen was used as a cryogenic media during a cryogenic turning environment. This was achieved using a cylinder with a capacity of 160 liters, along with a vacuum-insulated cryogenic decanting pipe and two copper nozzles, each with a diameter of 4 mm. The pressure and flow rate were maintained at 20 psi and 4 LPM, respectively. Dual nozzles, positioned at the flank and rake face, were employed to maximum efficiency [58]. Uncoated tungsten carbide inserts H13A (rhombic  $80^\circ$ ) mounted on tool holder "SCACL 1616 K 09-S" and used to perform turning experiments. Although coated inserts provide the benefits of high wear resistance, they also provide less heat dissipation, which is disadvantageous for Ti-6Al-4V due to their low thermal conductivity [59]. Less heat dissipation may affect the machined part's thermo-mechanical properties and surface integrity. The turning tool inserts have zero rack angle and  $7^\circ$  clearance angle with no chip breaker, which were chosen based on published work as well as on the recommendations of tool manufacture for Ti-6Al-4V. The actual machining setup, along with cutting inserts provided by SANDVIK COROMANT is shown in Figure 3.

Table 2. Chemical composition of Ti-6Al-4V

Chemical composition (%)					
Ti	V	Al	Fe	Cu	Cr
89.44	4.2	5.7	0.15	0.003	0.0023

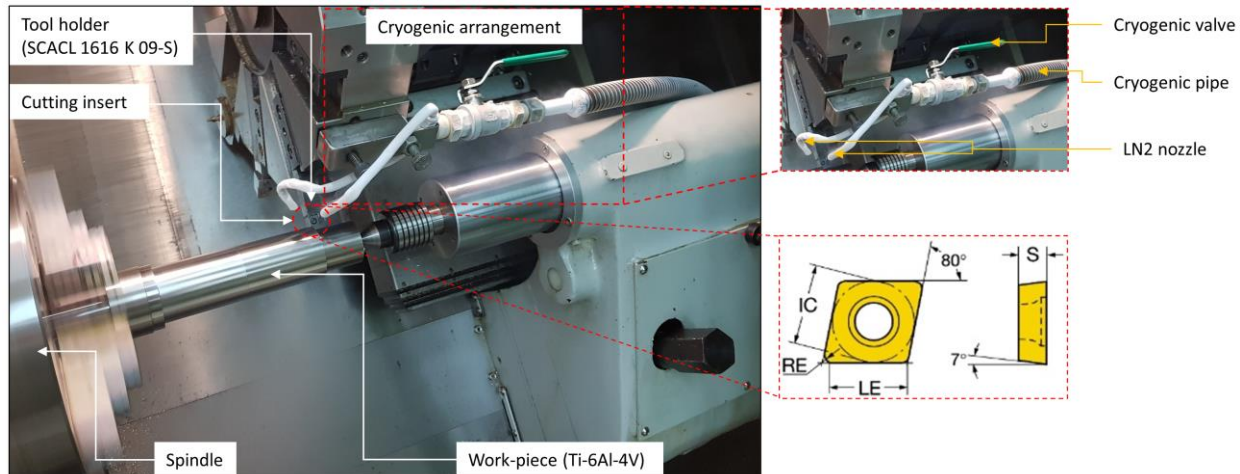


Figure 3. Actual machining setup

Table 3. Machine tool's specifications

ML-300 CNC Turning	
Manufacturer	YI-DA Precision Machinery Co., Ltd., Taiwan
Control	FANUC
Stroke	700 mm
Chuck diameter	300 mm (maximum)
Spindle power	15kW
Spindle speed	3300 rpm (maximum)
Total power	26kW

The turning experiments were performed under varying cutting speeds and tool feed rates, whereas the depth of cut was kept constant throughout both dry and cryogenic mediums. The parameter ranges were selected based on available literature [60], [61], ISO standards [62], and guidelines from the tool manufacturer [63]. These input parameters, along with their ranges, are depicted in Table 4. Experiments were performed according to the full factorial design of the experiment, as illustrated in Table 5, along with output responses. After execution of each experiment, the chips were dried and stored with care (in a plastic zipper bag) to obtain chip cross-section for chip morphology and shear angle calculations. Every plastic zipper bag is properly codified with cutting parameters immediately after the experiment is performed to avoid the shuffling of chips, which leads to destroying research goals. The research goal was to calculate shear angle and chip geometric features, which cannot be measured and analyzed directly from the workpiece. So, to get information about chip morphology, chip samples are first prepared. The standard route map shown in Figure 4 was chosen to prepare good samples such as hot mounting, grinding, polishing, and optical microscopy. A hydro-press mounting machine was used to hot mount chips in conductive Bakelite powder. Conductive Bakelite powder gives the advantage of exploring the samples in a scanning electron microscope (SEM), which will reduce the chance of any drift or charging during SEM analysis. Chips were bent in a V-shape so that they might not fall flat during powder pouring. After hot mounting, each sample was ground using waterproof silicon carbide grinding papers of grades P800, P1200, P2000, and P2400 to achieve a completely highlighted microstructure. The samples were mirror polished with 6, 3 and 1 microns diamond paste. The machine “PRESI Mecatech 264” was used for grinding polishing. Meiji MT-8530 metallurgical microscope was used to analyze the chip morphology under 10X and 20X magnification. The focused images were imported into the INFINITY software to get a calibrated scale.

Table 4. Input parameters and their ranges for the design of experiment

Parameters	Units	Range
Cutting speed-Vc	m/min	50, 75, 100, 125, 150
Tool feed rate-f	mm/rev	0.12, 0.16, 0.20, 0.24
Depth of cut-d	mm	1
Cutting medium		Dry Cryogenic

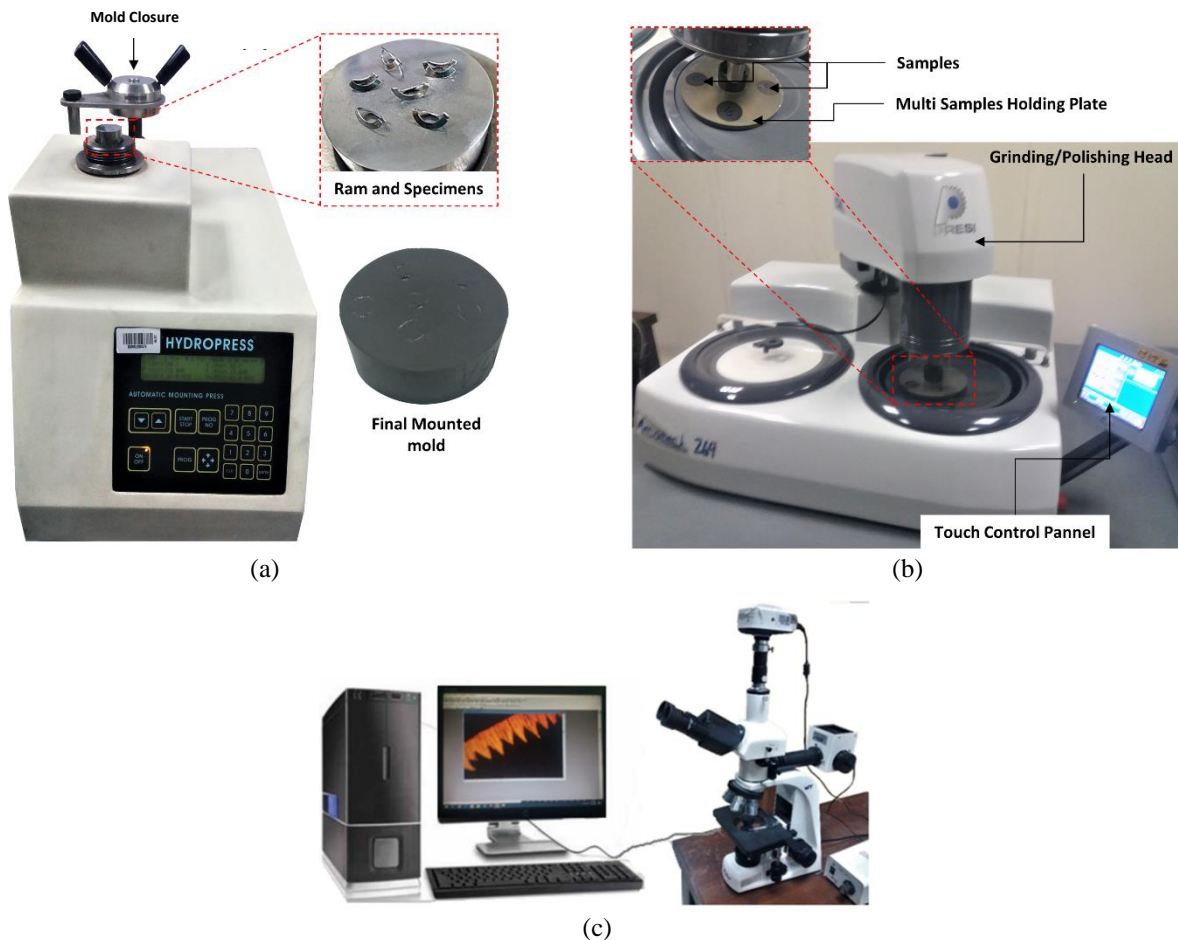


Figure 4. Route map followed for chip preparation: (a) chip mounting; (b) grinding and polishing; (c) optical microscopy

Table 5. Full factorial array for experimentation and corresponding morphological response parameters of segmented chips

Condition	Tool feed rate-f (mm/rev)	Cutting speed-V <sub>c</sub> (m/min)	Shear angle (φ)								Compression ratio (r')								Segmentation degree (Gs)	
			Model-1		Model-2		Model-3		Model-4		Model-1		Model-2		Model-3		Model-4		dry	cryo-genic
			dry	cryo-genic	dry	cryo-genic	dry	cryo-genic	dry	cryo-genic	dry	cryo-genic	dry	cryo-genic	dry	cryo-genic	dry	cryo-genic		
1	0.12	50	43	34	61	51	36.9	34.9	38.6	43.3	0.95	0.68	1.69	1.68	0.75	0.70	0.80	0.94	0.33	0.43
2	0.12	75	48	40	58	53	36.1	29.1	35.7	40.0	1.09	0.82	1.62	1.70	0.73	0.56	0.72	0.84	0.38	0.45
3	0.12	100	43	43	60	54	34.3	28.8	33.7	36.5	0.93	0.93	1.73	1.77	0.68	0.55	0.67	0.74	0.39	0.45
4	0.12	125	49	34	61	46	36.2	24.2	32.1	36.7	1.14	0.68	1.83	1.88	0.73	0.45	0.63	0.74	0.42	0.47
5	0.12	150	54	39	64	53	34.5	21.5	31.7	34.8	1.37	0.82	2.06	2.18	0.69	0.39	0.62	0.69	0.43	0.48
6	0.16	50	50	40	58	57	34.2	42.4	39.7	42.3	1.18	0.85	1.59	1.48	0.68	0.91	0.83	0.91	0.35	0.40
7	0.16	75	46	52	54	63	34.4	41.9	35.9	40.4	1.03	1.27	1.67	1.65	0.68	0.90	0.72	0.85	0.37	0.45
8	0.16	100	37	45	55	63	34.8	39.8	34.9	37.7	0.75	1.02	1.70	1.85	0.70	0.83	0.70	0.77	0.40	0.47
9	0.16	125	44	39	58	66	34.5	37.4	32.6	38.3	0.96	0.81	1.80	1.94	0.69	0.76	0.64	0.79	0.45	0.50
10	0.16	150	40	41	59	66	25.7	47.4	32.1	36.4	0.84	0.86	1.98	2.13	0.48	1.09	0.63	0.74	0.48	0.52
11	0.2	50	49	39	52	56	32.8	35.2	41.4	40.1	1.15	0.80	1.51	1.39	0.64	0.71	0.88	0.84	0.40	0.46
12	0.2	75	43	37	52	55	33.4	39.8	38.1	39.1	0.94	0.74	1.47	1.55	0.66	0.83	0.78	0.81	0.42	0.49
13	0.2	100	43	46	58	63	33.2	39.3	36.3	41.8	0.92	1.04	1.63	1.68	0.65	0.82	0.73	0.89	0.46	0.48
14	0.2	125	30	43	52	57	31.0	36.5	33.0	40.4	0.58	0.94	1.70	1.74	0.60	0.74	0.65	0.85	0.48	0.53
15	0.2	150	50	51	61	66	31.0	38.2	32.8	38.7	1.19	1.25	1.83	2.01	0.60	0.79	0.64	0.80	0.49	0.55
16	0.24	50	47	35	55	51	31.5	36.9	42.0	44.6	1.06	0.71	1.43	1.28	0.61	0.75	0.90	0.98	0.44	0.48
17	0.24	75	49	32	56	56	46.5	31.5	41.0	43.6	1.15	0.61	1.42	1.40	1.05	0.61	0.87	0.95	0.45	0.51
18	0.24	100	40	41	52	52	37.9	36.8	37.2	43.8	0.84	0.87	1.40	1.46	0.78	0.75	0.76	0.96	0.48	0.51
19	0.24	125	44	38	60	55	35.6	34.0	37.1	42.5	0.95	0.78	1.61	1.70	0.72	0.68	0.76	0.92	0.50	0.54
20	0.24	150	48	40	63	58	34.4	32.3	35.1	39.6	0.93	0.85	1.75	1.82	0.68	0.63	0.70	0.83	0.51	0.57

### 3.0 CHIP MORPHOLOGY PARAMETERS

The geometric parameters of each sample include the height of the peak ( $h_p$ ), the height of the valley ( $h_v$ ), complimentary angle ( $\theta'$ ), tooth pitch ( $P_c$ ), crack pitch ( $P$ ) shear angle ( $\phi$ ) and equivalent deformed chip thickness or segment length ( $d_{ch}$ ) etc. All these parameters (shown in Figure 5) are measured three times from different portions of the chip. Shear angle was calculated using all four methods mentioned, whereas chip compression ratio or chip shrinkage factor ( $r'$ ) practically and theoretically and chip segmentation degree ( $G_s$ ) were calculated using the following equations 1 to 5.

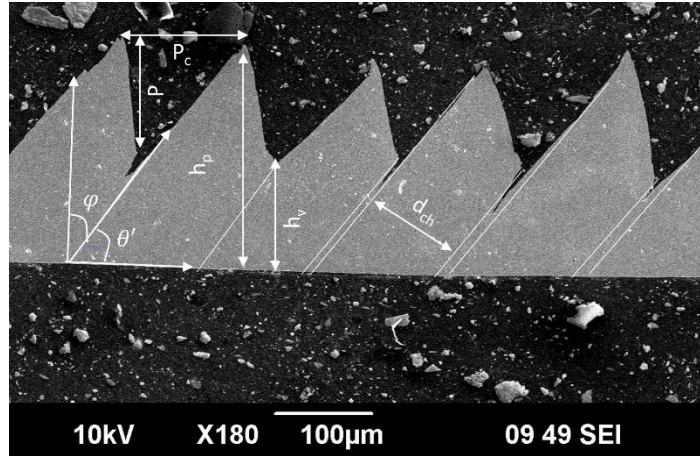


Figure 5. Geometric parameters of segmented chip in the present study

$$\text{Chip compression ratio-Theoretical-M1 } (r') = \frac{P_c}{P} \quad (1)$$

$$\text{Chip compression ratio-Theoretical-M2 } (r') = \frac{h_1}{h_2} \quad (2)$$

$$\text{Chip compression ratio-Theoretical-M3 } (r') = \frac{h_1}{h_2} \quad (3)$$

$$\text{Chip compression ratio-Practical-M4 } (r') = \frac{\sin \phi}{\cos(\phi - \gamma)} \quad (4)$$

$$\text{Chip segmentation degree } (G_s) = \frac{h_p - h_v}{h_p} \quad (5)$$

In equations 1 to 5,  $P_c$  is the tooth's pitch, and  $P$  is the crack pitch;  $h_1$  is uncut thickness, which is equal to the feed rate in single point turning;  $h_2$  is the deformed thickness (segment length)  $d_{ch}$  ( $t_c = \frac{h_p + h_v}{2}$ );  $\phi$  is the practically measured shear angle, and  $\gamma$  is the tool rack angle;  $h_p$  is the height of the peak; and  $h_v$  is the height of the valley.

### 4.0 RESULTS AND DISCUSSION

Under dry and cryogenic cutting conditions, serrated chips were created at all cutting speeds (50 m/min-150 m/min) and tool feed rates (0.12 mm/rev-0.24 mm/rev). Using the aforementioned relationships, the response parameters of serrated chips to a specific set of cutting settings for both cutting environments were determined and are shown in Table 5.

#### 4.1 Comparison of Shear Angle Model

The shear angle was calculated with models M1-3 (theoretical with continuous chip assumption) and model-4 (practically by subtracting the segmented angle from  $90^\circ$ ). Angles obtained from model-1 and model-2 are greater than  $45^\circ$  for both cutting environments, which is practically impossible according to Merchant's theory. Similar results were also reported by others [18],[28]. However, model-3 gives a shear angle less than or equal to  $45^\circ$ , which is under consideration, whereas model-4 is the actual measurement of the shear angle obtained experimentally from ground and polished chip samples. Thus, the results of both models (model-3 and model-4) for dry and cryogenic machining are graphically presented in Figure 6 and Figure 7, respectively. It can easily be noticed that there is a lot of deviation (highlighted in red circles) in the output of model-3 as compared to the output of model-4 (actual measurement), which appeals that continuous chip assumption can't represent the true chip formation process. In model-4, the shear angle oscillated from  $31.7^\circ$  to  $44.6^\circ$ , consistent with the findings of studies [50],[52],[64], which lies between the range highlighted in Stabler's theory of orthogonal cutting [53]. Thus, model-4, referred to by R. Komanduri et al. [55], is the

most appropriate model to calculate the shear angle for titanium alloy Ti-6Al-4V machining under dry and cryogenic cutting environments.

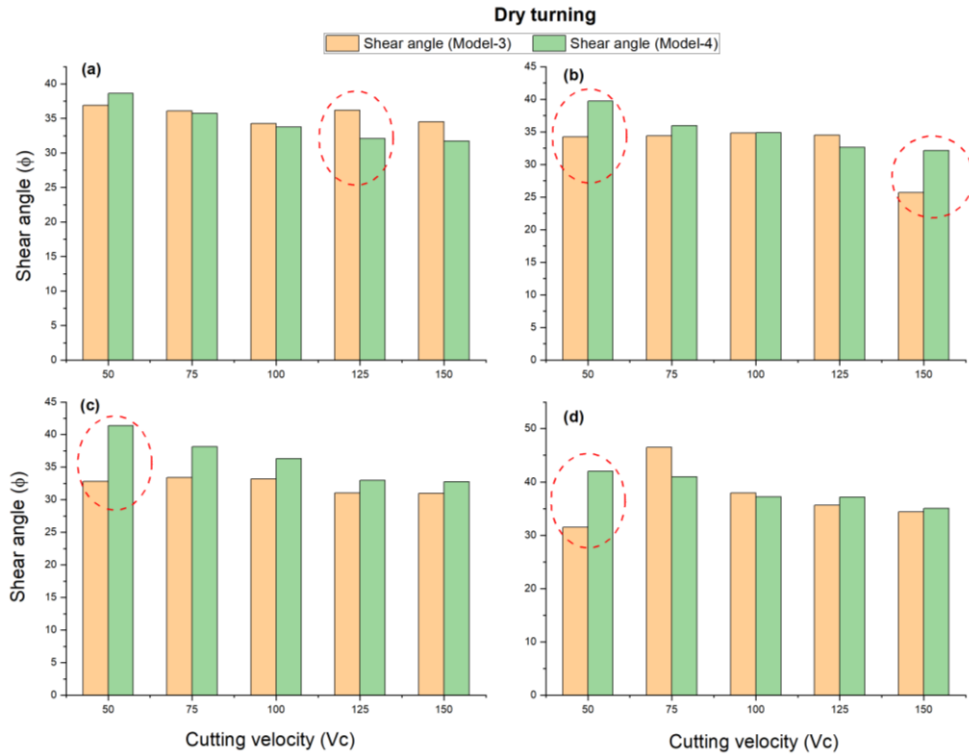


Figure 6. Comparison of shear angle model-3 and model-4 for dry turning: (a) 0.12 mm/rev tool feed rate; (b) 0.16 mm/rev tool feed rate; (c) 0.20 mm/rev tool feed rate; (d) 0.24 mm/rev tool feed rate

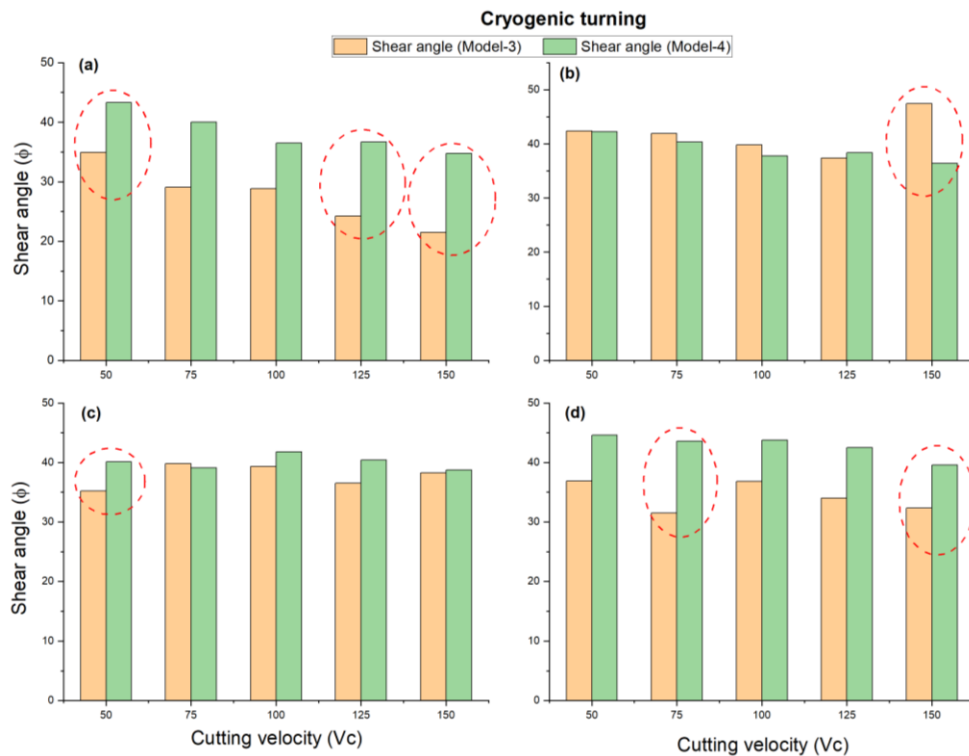


Figure 7. Comparison of shear angle model-3 and model-4 for cryogenic turning: (a) 0.12 mm/rev tool feed rate; (b) 0.16 mm/rev tool feed rate; (c) 0.20 mm/rev tool feed rate; (d) 0.24 mm/rev tool feed rate

#### 4.2 Effect of Cutting Speed and Feed Rate on Shear Angle

The effect of cutting speed and tool feed rate was examined for the shear angle obtained from model 4. The results are framed in the form of a line graph below in Figure 8. Shear angle values oscillate from 31.7° to 44.6°. The graph

reflects a decreasing trend of shear angle with an increase in cutting speed. Thus, a low shear angle is observed at elevated cutting speeds, yielding high cutting forces and energy for the defined machining conditions. This was attributed to the work hardening of the titanium alloy (Ti-6Al-4V) at elevated cutting speeds, which leads to a higher strain and shear plane area [65], [61], [66]. While it is directly proportional to the tool feed rate for both dry and cryogenic cutting mediums, this relationship yields a smaller shear plane, resulting in reduced cutting force and energy. This trend has been previously reported in the literature for the dry turning of Al-6061-T6 alloy [67]. The shear angle for cryogenic turning at all feed rates is greater than that for dry turning, which is advantageous for reducing cutting forces and energy consumption, and results were aligned with other studies [68], [69]. For dry and cryogenic turning, a maximum shear angle of  $42^\circ$  and  $44.6^\circ$  was observed at cutting speeds of 50 m/min speed and a feed rate of 0.24 mm/rev, respectively. The fluctuation in tool wear and the material's adiabatic shearing may be to blame for the scatter in the shear angle [34].

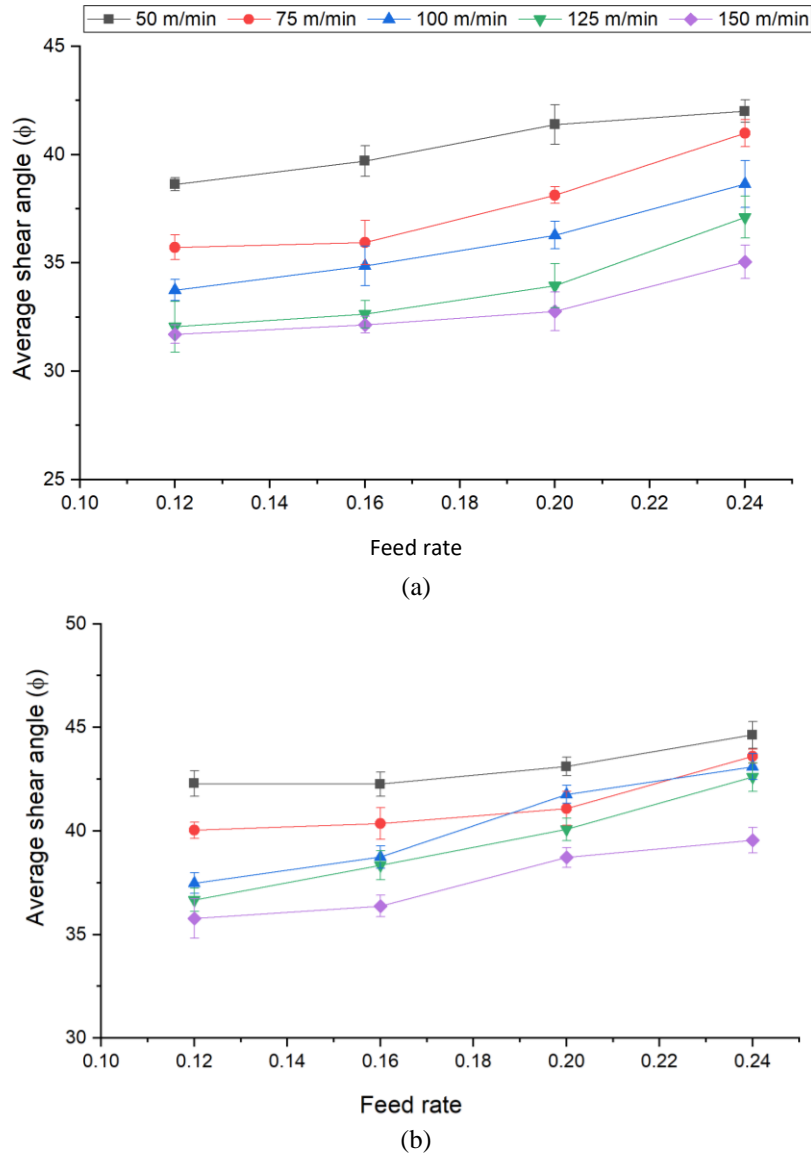


Figure 8. Effect of tool feed rate and cutting velocity on the average shear angle: (a) dry turning  
(b) cryogenic turning

#### 4.3 Effect of Cutting Medium on the Shear Angle

Cutting medium plays a vital role in the chip formation mechanism, which further affects the integrity and thermo-mechanical properties of the machined part, resulting from the distribution of residual tensile stresses. During the cutting process, the workpiece gets heated due to the friction created owing to the rubbing action of the tool and workpiece. Hence, the application of a cooling medium at that time is synonymous with the surface treatment, which may prove to alter the thermo-mechanical properties of the part. Thus, the shear angle of dry and cryogenics machining is compared under the respective sets of cutting conditions and tool feed rates, as shown in Figure 9. The shear angle was found to be superior for the cryogenic cutting medium as compared to dry cutting. The main reason for this occurrence is the reduced tool chip contact length [70], which leads to minimized work hardening effect and residual stresses due to lower temperature [66], [68]. It is also pertinent to highlight that chip compression ratio is also affected by tool chip contact length, which is another vital index for process sustainability and economy. Higher shear angle along with cryogenic

medium is a beneficial indication of enhanced dimensional accuracy, lowered surface roughness, and improved fatigue life of machined parts [56],[61]. Besides this, both angles are almost equal ( $41^\circ$ ) at a speed of 50 m/min and a tool feed rate of 0.2 mm/rev. Thus, a cryogenic cutting medium for titanium alloy Ti-6Al-4V for a defined set of feed rates and cutting speed is the most suitable; anyhow, a cutting speed of 50 m/min and a feed rate of 0.2 mm/rev can be applicable for both dry and cryogenic cutting medium.

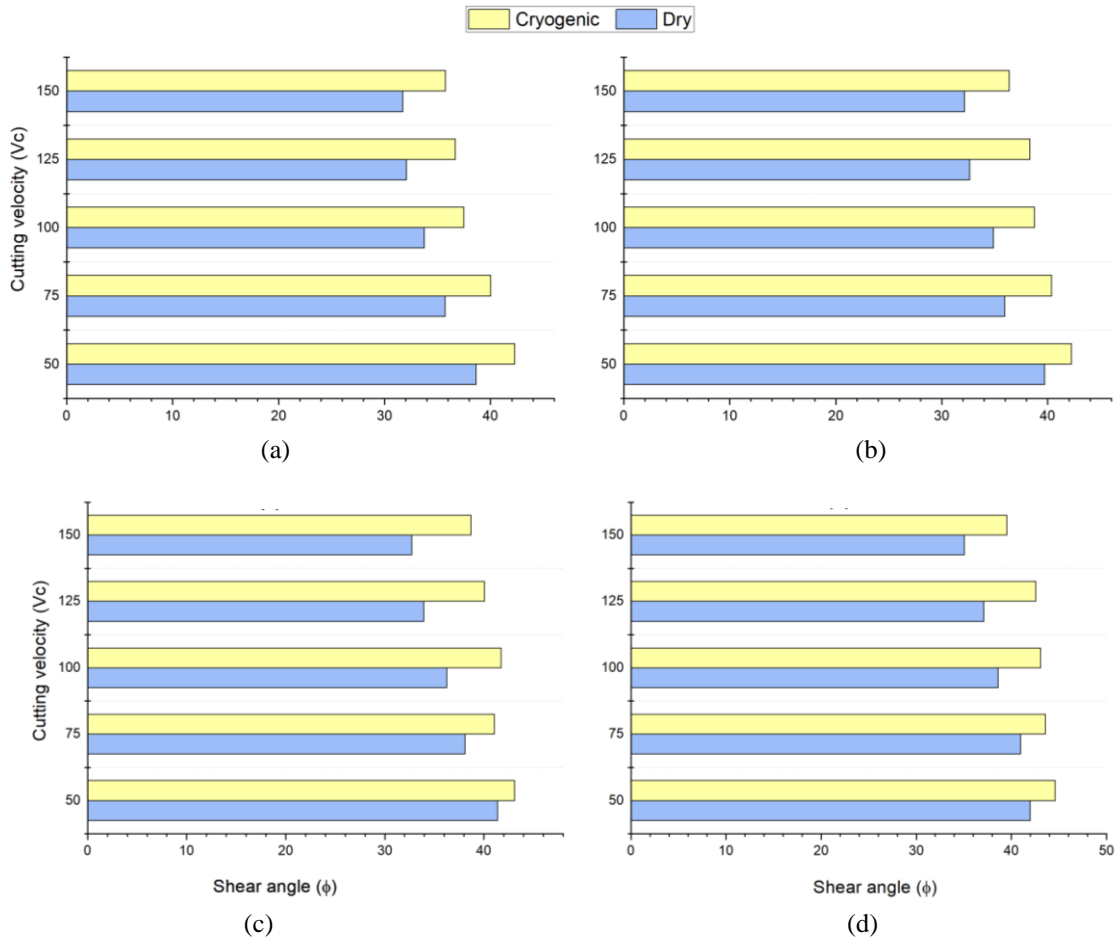


Figure 9. Effect of cutting medium on average shear angle: (a) 0.12 mm/rev tool feed rate; (b) 0.16 mm/rev tool feed rate; (c) 0.20 mm/rev tool feed rate; (d) 0.24 mm/rev tool feed rate

#### 4.4 Chip Compression Ratio ( $r'$ )

Chip compression ratio is also called the chip shrinkage factor, and it is used to estimate chip formation efficiency, forces, and energy consumption in the cutting process because it is interlinked with deformation in the machining process. It is the ratio of undeformed chip thickness to deformed chip thickness, and this ratio is always less than one in the metal-cutting process. As the deformed thickness (after the cut) becomes greater than before due to plastic deformation, the compression ratio for both mediums was calculated using theoretical approaches (Equations 1, 2, and 3) and practically using the actual calculated shear angle through Equation 4. The results are contrasted in Table 5. The compression ratio calculated theoretically through Equations 1 and 2 (model-1 and model-2) is greater than one which is practically not possible, whereas results acquired theoretically through Equation 3 (using mean peak and valley approach-M3 as undeformed thickness) are less than one which could be practically possible. Thus, the first two theoretical approaches were eliminated in the first attempt. The results of theoretical approach M3 and practical approach M4 are illustrated graphically below in Figure 10. Overall, the practically acquired compression ratio is directly proportional to the tool feed rate; the higher the feed rate, the lower the compression ratio. However, it has an inverse relation with cutting velocity for both cutting environments. The decrease in chip compression ratio with an increase in cutting speed was attributed to the decline in chip thickness. This decrease occurs as a result of the widening of the shear band, which tends to increase thermal conductivity. Thermal conductivity increases with the temperature of the cutting zone [71], and hence, the widening of the shear band with an increase in cutting speed results in a reduced chip compression ratio [56], [61].

Nevertheless, the theoretically calculated compression ratio using approach model-3 shows some irregular trends, and its value is also greater than one (encircled in Figure 10) at 75 mm/min, 0.24 mm/rev in the dry medium, and at 150 mm/min, 0.16 mm/rev in the cryogenic medium. This suggests that the theoretical model may be unreliable. Therefore, the most appropriate approach to estimating the segmented chip compression ratio is the practical approach (Equation 4) using the practically calculated shear angle.

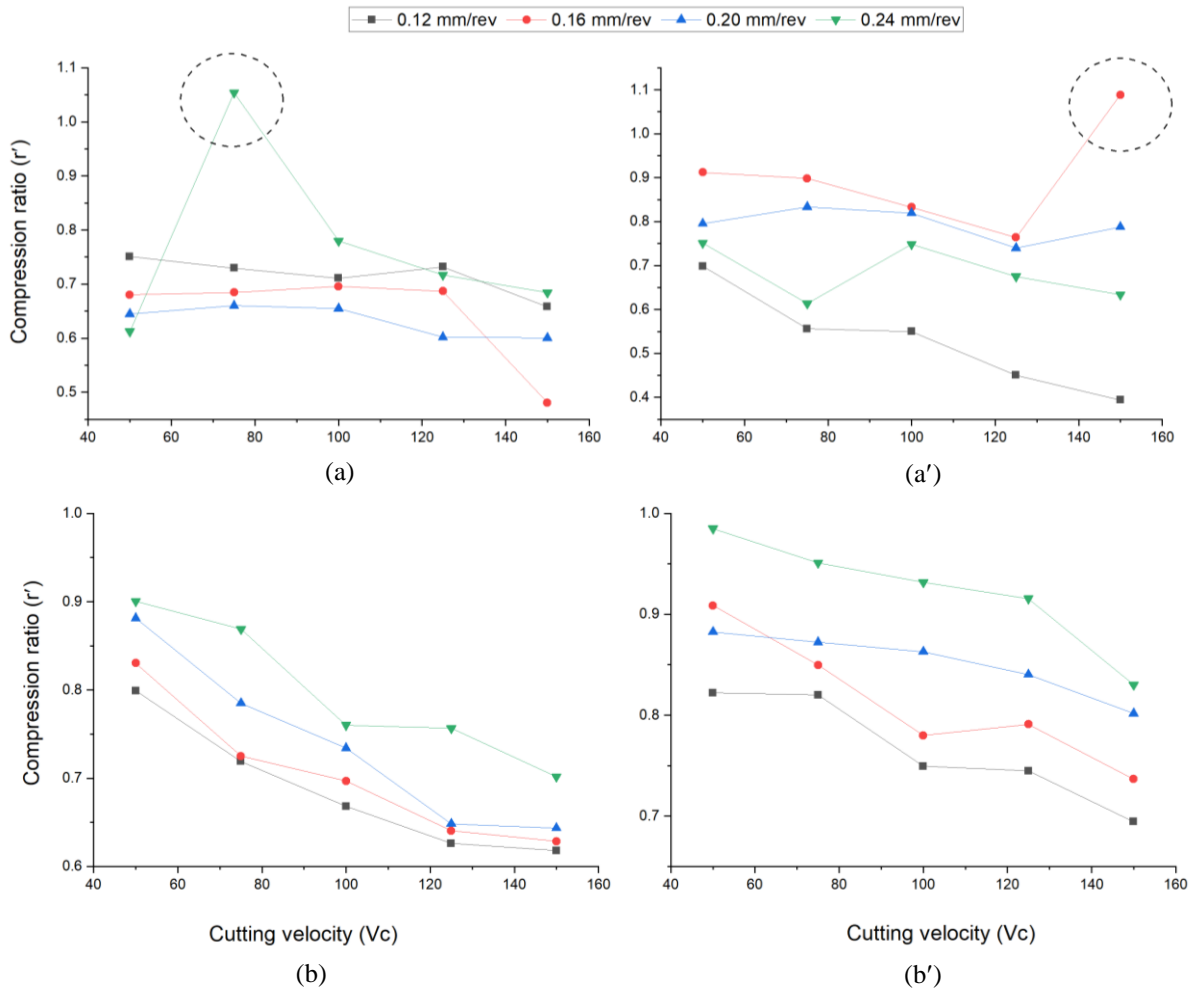


Figure 10. Effect of cutting velocity and tool feed rate on chip compression ratio: (a, a') theoretical dry-cryogenic; (b, b') practical dry-cryogenic

#### 4.5 Chip Segmentation Degree ( $G_s$ )

The degree of chip deformation, also known as height ratio, is calculated by Equation 5 using the chip peak and valley heights. It should always be less than one for the segmented chip, and once it reaches the value of one, the segmented chip transforms into a continuous chip. Figure 11 depicts the effect of cutting speed vs tool feed rate on the degree of chip segmentation for dry and cryogenic machining, respectively. Initially, at feed rates of 0.12 and 0.16, the segmentation degree dramatically increases, whereas, at feed rates of 0.2 and 0.24, it increases slowly. Overall, it can be noticed that the segmentation degree increases linearly with an increase in both feed rate and cutting speed, which agrees with the trends reported by other researchers [18],[27],[34],[50],[69]. Overall, the chip segmentation degree in cryogenic machining was higher than in dry machining, indicating a shorter contact length between the tool and chip. This characteristic is advantageous for improving tool life and reducing energy consumption. This shows that contact length between the segments gradually decreases, leading to the more prominent and regular deformation of the adiabatic shear zone [69]. This is due to the fact that the cracking of the adiabatic shear band reduces the connecting area between the chips. Microscopic illustrations of segments at constant feed rate (0.2 mm/rev) and varying cutting speed (50 m/min-150 m/min) for both dry and cryogenic machining are summarized in Figure 12.

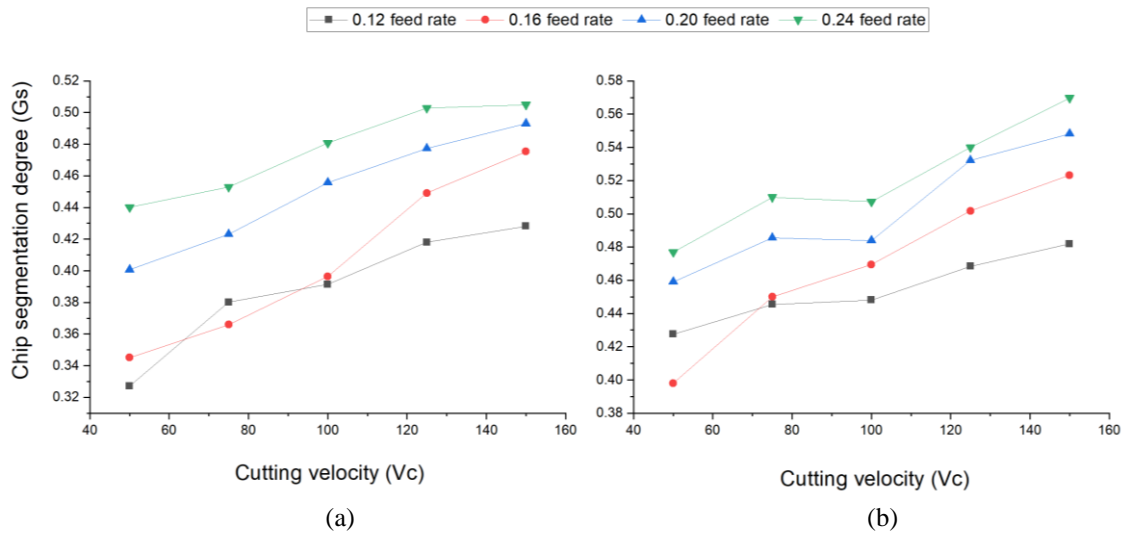


Figure 11. Effect of cutting velocity and tool feed rate on chip segmentation degree: (a) dry turning; (b) cryogenic turning

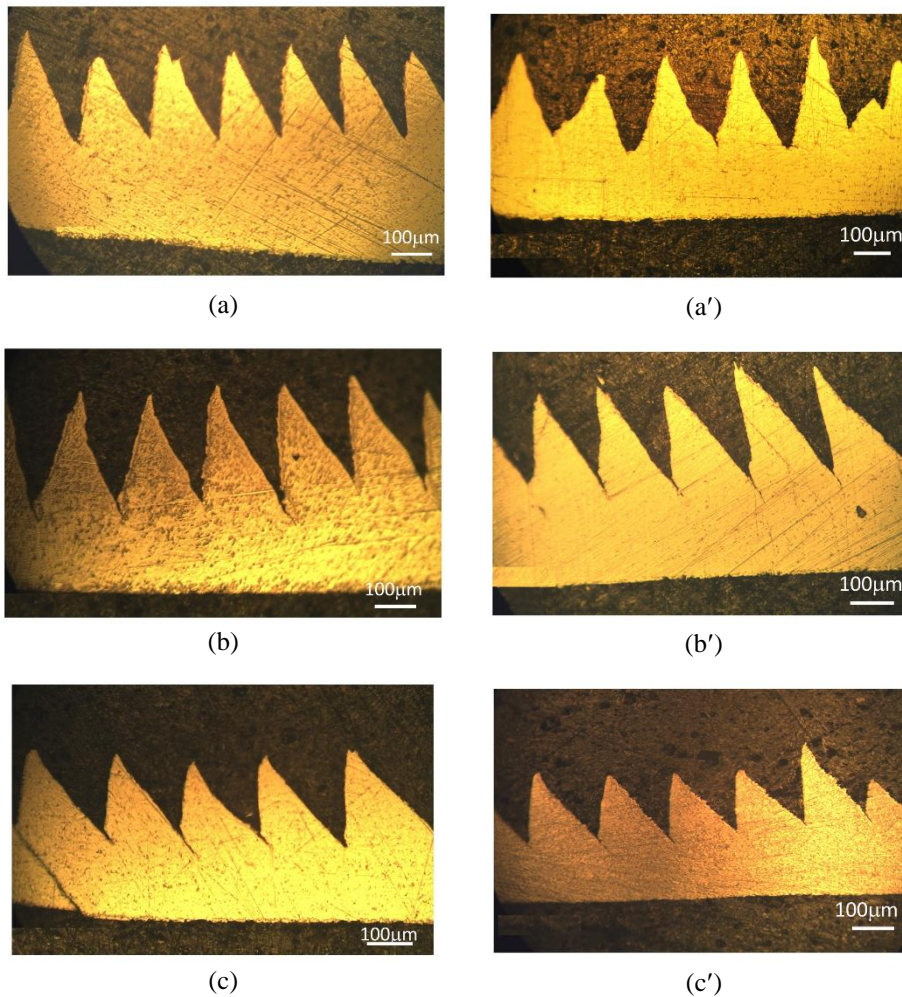


Figure 12. Microscopic illustration of segments at constant tool feed rate (0.20 mm/rev) and varying cutting speed: (a-a') dry-cryogenic at 50 m/min; (b-b') dry-cryogenic at 75 m/min; (c-c') dry-cryogenic at 100 m/min

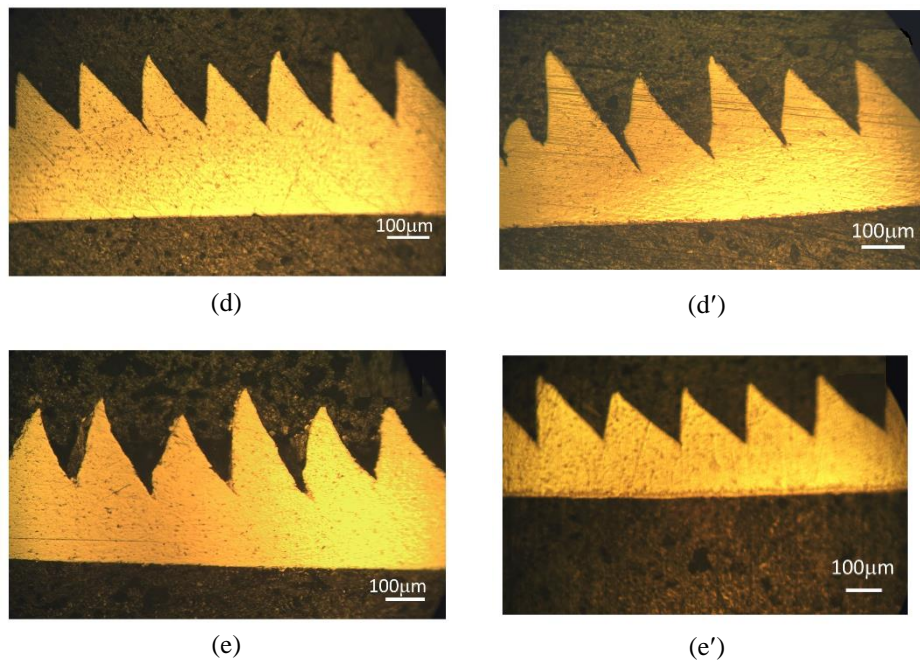


Figure 12. (cont.) (d-d') dry-cryogenic at 125 m/min; (e-e') dry-cryogenic at 150 m/min

## 5.0 CONCLUSIONS

In this research, the chips (obtained in single point turning of Ti-6Al-4V under dry and cryogenic medium) were experimentally analyzed for a selected set of cutting speeds (50 m/min-150 m/min) and feed rate (0.12 mm/rev-0.24 mm/rev). Based on results and discussions, the following conclusions may possibly be inferred:

- Theoretical or chip thickness models can't show the true chip formation process. Thus, method 4 (experimentally measured) is the most suitable method to calculate the shear angle for titanium alloy Ti-6Al-4V.
- Experimentally measured shear angle has a decreasing trend with an increase in cutting speed, and it has a linearly increased trend with an increase in feed rate.
- The shear angle in dry turning lies between  $31.7^\circ$  to  $42^\circ$  and cryogenic turning lies between  $34.8^\circ$  to  $44.6^\circ$ .
- The shear angle was observed to be higher for defined tool feed rates and cutting speeds in cryogenic turning compared to dry turning. This higher shear angle in cryogenic medium contributes to minimizing the work hardening effect and residual stresses due to the lower temperatures involved, which is advantageous for enhancing tool life and reducing energy consumption. It can be said that a larger shear angle is better because of the lower shear plane area and reduced cutting forces.
- The compression ratio is directly proportional to the tool feed rate but inversely proportional to the cutting speed. Segmented chips can be calculated using a practically obtained shear angle rather than the theoretically calculated thickness approach.
- The chip segmentation degree in both environments was less than one, which shows a segmented chip formation agreement. It showed a linearly direct relation between cutting speed and feed rate.

## 6.0 ACKNOWLEDGEMENT

The authors would like to thank the Department of Design and Manufacturing Engineering, National University Sciences and Technology, NUST, Islamabad, Pakistan, for providing the facility to conduct research.

## 7.0 REFERENCES

- [1] M.C. Howard, "Sustainable Manufacturing Initiative (SMI): A True Public-Private Dialogue," *The US Department of Commerce*, 2019. <https://www.manufacturing.gov/sustainability> (accessed Mar. 03, 2023).
- [2] N. Khanna, G. Kshitij, M. Solanki, T. Bhatt, O. Patel, A. Uysal et al., "In pursuit of sustainability in machining thin walled  $\alpha$ -titanium tubes: An industry supported study," *Sustainable Materials and Technologies*, vol. 36, p. e00647, 2023.
- [3] G.Y. Zhao, Z.Y. Liu, Y. He, H.J. Cao, and Y.B. Guo, "Energy consumption in machining: Classification, prediction, and reduction strategy," *Energy*, vol. 133, pp. 142–157, 2017.
- [4] S.S. Warsi, M.H. Agha, R. Ahmad, S.H.I. Jaffery, and M. Khan, "Sustainable turning using multi-objective optimization: A study of Al 6061 T6 at high cutting speeds," *International Journal of Advanced Manufacturing Technology*, vol. 100, pp. 843–855, 2019.

- [5] M. Khan, S.S. Warsi, S.H.I. Jaffery, R. Ahmad, and M. Younas, "Analysis of Energy Consumption in Orthogonal Machining of Al 6061-T6 Alloy," in *Advances in Manufacturing Technology XXXIII: Proceedings of the 17th International Conference on Manufacturing Research, incorporating the 34th National Conference on Manufacturing Research, 10-12 September 2019, Queen's University, Belfast*, 2019, vol. 9, p. 327.
- [6] D. Liu, C. Ni, Y. Wang, and L. Zhu, "Review of serrated chip characteristics and formation mechanism from conventional to additively manufactured titanium alloys," *Journal of Alloys and Compounds*, vol. 970, p. 172573, 2024.
- [7] M.U. Farooq, S. Anwar, and A. Hurairah, "Reducing micro-machining errors during electric discharge machining of titanium alloy using nonionic liquids," *Materials and Manufacturing Processes*, vol. 39, no. 4, pp. 449–464, 2024.
- [8] M.U. Farooq, M.A. Ali, Y. He, A.M. Khan, C.I. Pruncu, M. Kashif et al., "Curved profiles machining of Ti6Al4V alloy through WEDM: investigations on geometrical errors," *Journal of Materials Research and Technology*, vol. 9, no. 6, pp. 16186–16201, 2020.
- [9] X. Li, X. Zhang, H. Zhang, J. Yang, A.B. Nia, and G.B. Chai, "Mechanical behaviors of Ti/CFRP/Ti laminates with different surface treatments of titanium sheets," *Composite Structures*, vol. 163, pp. 21–31, 2017.
- [10] D. Chauhan, M.A. Makhesana, R.A.R. Rashid, V. Joshi, and N. Khanna, "Comparison of Machining Performance of Ti-6Al-4V under Dry and Cryogenic Techniques Based on Tool Wear, Surface Roughness, and Power Consumption," *Lubricants*, vol. 11, no. 11, 2023.
- [11] S. Pervaiz, N. Ahmad, K. Ishfaq, S. Khan, I. Deiab, and S. Kannan, "Implementation of sustainable vegetable-oil-based Minimum Quantity Cooling Lubrication (MQCL) machining of titanium alloy with coated tools," *Lubricants*, vol. 10, no. 10, 2022.
- [12] M. Nouari and H. Makich, "Analysis of physical cutting mechanisms and their effects on the tool wear and chip formation process when machining aeronautical titanium alloys: Ti-6Al-4V and Ti-55531," *Machining of titanium alloys*, Springer, 2014, pp. 79–111.
- [13] N. Ahmed, S. Anwar, K. Ishfaq, M. Rafaqat, M. Saleh, and S. Ahmad, "The potentiality of sinking EDM for micro-impressions on Ti-6Al-4V: keeping the geometrical errors (axial and radial) and other machining measures (tool erosion and work roughness) at minimum," *Scientific Reports*, vol. 9, no. 1, p. 17218, 2019.
- [14] A. Hosseini and H.A. Kishawy, "Cutting Tool Materials and Tool Wear," in *Machining of Titanium Alloys*, pp. 31–56, 2014. Materials Forming, Machining and Tribology. Springer, Berlin, Heidelberg.
- [15] H. El-Hofy, *Fundamentals of machining processes: conventional and nonconventional processes*. CRC press, 2018.
- [16] N. K. Gupta, N. Somani, C. Prakash, R. Singh, A.S. Walia, S. Singh et al., "Revealing the WEDM process parameters for the machining of pure and heat-treated titanium (Ti-6Al-4V) alloy," *Materials*, vol. 14, no. 9, p. 2292, 2021.
- [17] A. Festas, A. Ramos, and J. P. Davim, "Machining of titanium alloys for medical application-a review," in *Proceedings of the Institution of Mechanical Engineers, Part B: Journal of Engineering Manufacture*, vol. 236, no. 4, pp. 309–318, 2022.
- [18] S. Carvalho, A. Horovistiz, and J. P. Davim, "Morphological characterization of chip segmentation in Ti-6Al-7Nb machining: A novel method based on digital image processing," *Measurement: Journal of the International Measurement Confederation*, vol. 206, p. 112330, 2023.
- [19] S. L. Semiatin and S. B. Rao, "Shear localization during metal cutting," *Materials Science and Engineering*, vol. 61, no. 2, pp. 185–192, 1983.
- [20] A. Molinari, C. Musquar, and G. Sutter, "Adiabatic shear banding in high speed machining of Ti-6Al-4V: Experiments and modeling," *International Journal of Plasticity*, vol. 18, no. 4, pp. 443–459, 2002.
- [21] G. Sutter, "Chip geometries during high-speed machining for orthogonal cutting conditions," *International Journal of Machine Tools and Manufacture*, vol. 45, no. 6, pp. 719–726, 2005.
- [22] S. S. Joshi, N. Ramakrishnan, and P. Ramakrishnan, "Micro-structural analysis of chip formation during orthogonal machining of Al/SiCp composites," *Journal of Engineering Materials and Technology*, vol. 123, no. 3, pp. 315–321, 2001.
- [23] R. Komanduri, T. Schroeder, J. Hazra, B.F. Von Turkovich, and D.G. Flom, "On the catastrophic shear instability in high-speed machining of an AISI 4340 steel," *Journal of Manufacturing Science and Engineering*, vol. 104, no. 2, pp. 121–131, 1982.
- [24] M.A. Elbestawi, A.K. Srivastava, and T.I. El-Wardany, "A model for chip formation during machining of hardened steel," *CIRP Annals*, vol. 45, no. 1, pp. 71–76, 1996.
- [25] M. C. Shaw and A. Vyas, "Chip formation in the machining of hardened steel," *CIRP Annals*, vol. 42, no. 1, pp. 29–33, 1993.
- [26] K. Nakayama, M. Arai, and T. Kanda, "Machining characteristics of hard materials," *CIRP Annals*, vol. 37, no. 1, pp. 89–92, 1988.
- [27] B. Wang and Z. Liu, "Serrated chip formation mechanism based on mixed mode of ductile fracture and adiabatic shear," *Proceedings of the Institution of Mechanical Engineers, Part B: Journal of Engineering Manufacture*, vol. 228, no. 2, pp. 181–190, 2014.
- [28] S. Sun, M. Brandt, and M. S. Dargusch, "Effect of tool wear on chip formation during dry machining of Ti-6Al-4V alloy, part 1: Effect of gradual tool wear evolution," *Proceedings of the Institution of Mechanical Engineers, Part B: Journal of Engineering Manufacture*, vol. 231, no. 9, pp. 1559–1574, 2017.
- [29] M. P. Groover, *Fundamentals of modern manufacturing: Materials, processes, and systems*. John Wiley & Sons, 2020.
- [30] M. E. Merchant, "Mechanics of the metal cutting process. I. Orthogonal cutting and a type 2 chip," *Journal of Applied Physics*, vol. 16, no. 5, pp. 267–275, 1945.

- [31] D. A. Stephensen, "Material characterization for metal-cutting force modeling," *Journal of Engineering Materials and Technology*, vol. 111, no. 2, pp. 210-219, 1989.
- [32] S. Joshi, A. Tewari, and S.S. Joshi, "Microstructural characterization of chip segmentation under different machining environments in orthogonal machining of Ti6Al4V," *Journal of Engineering Materials and Technology*, vol. 137, no. 1, p. 11005, 2015.
- [33] D.M. Turlay, E.D. Doyle, and S. Ramalingam, "Calculation of shear strains in chip formation in titanium," *Materials Science and Engineering*, vol. 55, no. 1, pp. 45-48, 1982.
- [34] W. Bai, R. Sun, A. Roy, and V. V. Silberschmidt, "Improved analytical prediction of chip formation in orthogonal cutting of titanium alloy Ti6Al4V," *International Journal of Mechanical Sciences*, vol. 133, pp. 357-367, 2017.
- [35] S. Joshi, "Dimensional inequalities in chip segments of titanium alloys," *Engineering Science and Technology, an International Journal*, vol. 21, no. 2, pp. 238-244, 2018.
- [36] M. Calamaz, D. Coupard, and F. Girot, "A new material model for 2D numerical simulation of serrated chip formation when machining titanium alloy Ti-6Al-4V," *International Journal of Machine Tools and Manufacture*, vol. 48, no. 3-4, pp. 275-288, 2008.
- [37] J. Hua and R. Shivpuri, "Prediction of chip morphology and segmentation during the machining of titanium alloys," *Journal of Materials Processing Technology*, vol. 150, no. 1-2, pp. 124-133, 2004.
- [38] C. Gao and L. Zhang, "Effect of cutting conditions on the serrated chip formation in high-speed cutting," *Machine Learning: Science and Technology*, vol. 17, no. 1, pp. 26-40, 2013.
- [39] M. Ba" ker, J. Ro" sler, and C. Siemers, "Finite element simulation of segmented chip formation of Ti6Al4V," *Journal of Manufacturing Science and Engineering*, vol. 124, no. 2, pp. 485-488, 2002.
- [40] Y. Zhang, J.C. Outeiro, and T. Mabrouki, "On the selection of Johnson-Cook constitutive model parameters for Ti-6Al-4 V using three types of numerical models of orthogonal cutting," *Procedia CIRP*, vol. 31, pp. 112-117, 2015.
- [41] B. Wang and Z. Liu, "Shear localization sensitivity analysis for Johnson-Cook constitutive parameters on serrated chips in high speed machining of Ti6Al4V," *Simulation Modelling Practice and Theory*, vol. 55, pp. 63-76, 2015.
- [42] F. Ducobu, E. Rivière-Lorphèvre, and E. Filippi, "Material constitutive model and chip separation criterion influence on the modeling of Ti6Al4V machining with experimental validation in strictly orthogonal cutting condition," *International Journal of Mechanical Sciences*, vol. 107, pp. 136-149, 2016.
- [43] M. Calamaz, D. Coupard, and F. Girot, "Numerical simulation of titanium alloy dry machining with a strain softening constitutive law," *Machine Learning: Science and Technology*, vol. 14, no. 2, pp. 244-257, 2010.
- [44] A. Vyas and M.C. Shaw, "Mechanics of saw-tooth chip formation in metal cutting," *Journal of Manufacturing Science and Engineering*, vol. 121, no. 2, pp. 163-172, 1999.
- [45] V. Upadhyay, P.K. Jain, and N.K. Mehta, "Comprehensive study of chip morphology in turning of Ti-6Al-4V," in *5th International & 26th All India Manufacturing Technology, Design and Research Conference*, 2014, pp. 2-7.
- [46] S.A. Iqbal, P.T. Mativenga, and M.A. Sheikh, "A comparative study of the tool-chip contact length in turning of two engineering alloys for a wide range of cutting speeds," *International Journal of Advanced Manufacturing Technology*, vol. 42, no. 1-2, pp. 30-40, 2009.
- [47] G.G. Ye, S.F. Xue, W. Ma, M.Q. Jiang, Z. Ling, X.H. Tong et al., "Cutting AISI 1045 steel at very high speeds," *International Journal of Machine Tools and Manufacture*, vol. 56, pp. 1-9, 2012.
- [48] A. Gente and H. W. Hoffmeister, "Chip formation in machining Ti6Al4V at extremely high cutting speeds," *CIRP Annals - Manufacturing Technology*, vol. 50, no. 1, pp. 49-52, 2001.
- [49] Q. Ke, D. Xu, and D. Xiong, "Cutting zone area and chip morphology in high-speed cutting of titanium alloy Ti-6Al-4V," *Journal of Mechanical Science and Technology*, vol. 31, no. 1, pp. 309-316, 2017.
- [50] Y.S. Hernández, F.J.T. Vilches, C.B. Gamboa, and L.S. Hurtado, "Experimental parametric relationships for chip geometry in dry machining of the Ti6Al4V alloy," *Materials (Basel)*, vol. 10, no. 7, 2018.
- [51] A.S. Siju, S. Jose, and S.D. Waigaonkar, "Experimental analysis and characterisation of chip segmentation in dry machining of Ti-6Al-4V alloy using inserts with hybrid textures," *CIRP Journal of Manufacturing Science and Technology*, vol. 36, pp. 213-226, 2022.
- [52] J. Lu, R. Khawarizmi, M. Monclús, J. Molina-Aldareguia, P. Kwon, and T.R. Bieler, "Effect of cutting speed on shear band formation and chip morphology of Ti-6Al-4V alloy using nanoindentation and EBSD mapping," *Materials Science and Engineering: A*, vol. 862, no. November 2022, p. 144372, 2023.
- [53] W. Grzesik, *Advanced machining processes of metallic materials: theory, modelling and applications*. Elsevier, 2008.
- [54] R. Komanduri, "Some clarifications on the mechanics of chip formation when machining titanium alloys," *Wear*, vol. 76, no. 1, pp. 15-34, Feb. 1982.
- [55] R. Komanduri and B.F. Von Turkovich, "New observations on the mechanism of chip formation when machining titanium alloys," *Wear*, vol. 69, no. 2, pp. 179-188, 1981.
- [56] M. Younas, S.H.I. Jaffery, A. Khan, and M. Khan, "Development and analysis of tool wear and energy consumption maps for turning of titanium alloy (Ti6Al4V)," *Journal of Manufacturing Processes*, vol. 62, pp. 613-622, 2021.
- [57] G.W.A. Kui, S. Islam, M.M. Reddy, N. Khandoker, and V.L.C. Chen, *Recent progress and evolution of coolant usages in conventional machining methods: A comprehensive review*, vol. 119, no. 1-2. Springer London, 2022.

- [58] M. Mia, M.K. Gupta, J.A. Lozano, D. Carou, D.Y. Pimenov, G. Królczyk et al., “Multi-objective optimization and life cycle assessment of eco-friendly cryogenic N<sub>2</sub> assisted turning of Ti-6Al-4V,” *Journal of Cleaner Production*, vol. 210, pp. 121–133, 2019.
- [59] S. Anwar, N. Ahmed, S. Pervaiz, S. Ahmad, A. Mohammad, and M. Saleh, “On the turning of electron beam melted gamma-TiAl with coated and uncoated tools: A machinability analysis,” *Journal of Materials Processing Technology*, vol. 282, 2020.
- [60] M.A. Khan, S.H.I. Jaffery, M. Khan, M. Younas, S.I. Butt, R. Ahmad et al., “Statistical analysis of energy consumption, tool wear and surface roughness in machining of Titanium alloy (Ti-6Al-4V) under dry, wet and cryogenic conditions,” *Mechanical Sciences*, vol. 10, no. 2, pp. 561–573, 2019.
- [61] M.A. Khan, S.H.I. Jaffery, and M. Khan, “Assessment of sustainability of machining Ti-6Al-4V under cryogenic condition using energy map approach,” *Engineering Science and Technology, an International Journal*, vol. 41, p. 101357, 2023.
- [62] “ISO Standard (1993) ‘ISO-3685,’ Tool-life Testing with Single Point Turning Tools.” 1993. [Online]. Available: ISO Standard (1993) <https://www.iso.org/standard/9151.html>
- [63] “Sandvik-Coromant, Product Catalogue, Turning tools,” 2015. <https://www.sandvik.coromant.com/en-us/tools/turning-tools>
- [64] G.G. Ye, S.F. Xue, M.Q. Jiang, X.H. Tong, and L.H. Dai, “Modeling periodic adiabatic shear band evolution during high speed machining Ti-6Al-4V alloy,” *International Journal of Plasticity*, vol. 40, pp. 39–55, 2013.
- [65] S. Sun, M. Brandt, and M.S. Dargusch, “Characteristics of cutting forces and chip formation in machining of titanium alloys,” *International Journal of Machine Tools and Manufacture*, vol. 49, no. 7–8, pp. 561–568, 2009.
- [66] I. Nouzil, S. Pervaiz, and S. Kannan, “Role of jet radius and jet location in cryogenic machining of Inconel 718: A finite element method based approach,” *International Journal on Interactive Design and Manufacturing*, vol. 15, pp. 1–19, 2021.
- [67] S. S. Warsi et al., “Development of energy consumption map for orthogonal machining of Al 6061-T6 alloy,” *The Proceedings of the Institution of Mechanical Engineers, Part B: Journal of Engineering Manufacture*, vol. 232, no. 14, pp. 2510–2522, 2018.
- [68] M.A. Khan, S.H.I. Jaffery, A.A. Baqai, and M. Khan, “Comparative analysis of tool wear progression of dry and cryogenic turning of titanium alloy Ti-6Al-4V under low, moderate and high tool wear conditions,” *International Journal of Advanced Manufacturing Technology*, vol. 121, no. 1, pp. 1269–1287, 2022.
- [69] W. Zhao, L. Gong, F. Ren, L. Li, Q. Xu, and A. M. Khan, “Experimental study on chip deformation of Ti-6Al-4V titanium alloy in cryogenic cutting,” *International Journal of Advanced Manufacturing Technology*, vol. 96, no. 9–12, pp. 4021–4027, 2018.
- [70] T. H. C. Childs, “Friction modelling in metal cutting,” *Wear*, vol. 260, no. 3, pp. 310–318, 2006.
- [71] K. Palanikumar, S. B. Boppana, and E. Natarajan, “Analysis of chip formation and temperature measurement in machining of titanium alloy (Ti-6Al-4V),” *Experimental Techniques*, vol. 47, no. 2, pp. 517–529, 2023.